

New Probe of the Electronic Structure of Amorphous Materials

Maria Strømme,¹ Rajeev Ahuja,² and Gunnar A. Niklasson^{1,*}

¹Department of Engineering Sciences, The Ångström Laboratory, Uppsala University, P.O. Box 534, SE-75121 Uppsala, Sweden

²Condensed Matter Theory, Department of Physics, Uppsala University, P.O. Box 530, SE-75121 Uppsala, Sweden

(Received 6 February 2004; published 12 November 2004)

Here we show that electrochemical equilibrium voltage curves of amorphous WO₃ and TiO₂ coatings exhibit fine structure in striking agreement with the density of states in the conduction bands, as obtained by *ab initio* calculations for the crystalline counterparts. We suggest that localization of the band states is essential for observing the electronic structure. Our highly sensitive electrochemical method opens new vistas for studying the electronic structure of nonmetallic disordered materials that can be intercalated with an ionic species.

DOI: 10.1103/PhysRevLett.93.206403

PACS numbers: 71.23.-k, 71.15.-m

Detailed knowledge of the electronic structure of amorphous and nanocrystalline materials is necessary for understanding their physical properties. *Ab initio* calculations [1–4] of the electron structure of amorphous materials are difficult and limited to small clusters [5]. There exists a need for accurate experimental techniques to probe the disorder-induced localized states close to the band edges, which are of prime importance for many physical properties [6,7]. Electron and x-ray spectroscopic methods have led to great advances in the experimental study of the electron band structure of, for example, transition metal compounds [8]. A number of electrical methods for studying the localized density of states in the band gap of amorphous semiconductors have also been extensively used [7,9], for example, deep level transient spectroscopy [10], but none of these are of general applicability. Optical absorption measurements can be used to study localized band tail states [11]. The electrochemical method, intercalation spectroscopy, which we propose in this Letter, is highly sensitive and convenient for studying the density of states in the lower part of the conduction band. Small ions (protons or alkali ions) are intercalated electrochemically into the material. To ensure charge balance, electrons are inserted together with the ions, which leads to filling of previously empty states. If the rigid-band approximation holds, the energy distribution of the inserted electrons will image the density of states in the conduction band. Alternatively, in compounds where ions can be extracted, an image of the valence band can be obtained. In order to validate the method, we compare electrochemical measurements, using chronopotentiometry, with state-of-the-art band structure computations for two of the most commonly used intercalation materials [12–15], namely, tungsten trioxide and titanium dioxide. In our investigation we used x-ray amorphous thin films, produced by sputter deposition [16]. Polycrystalline tungsten oxide films were studied for comparison [17].

Electrochemical measurements were performed in a standard three-electrode arrangement with the film serv-

ing as working electrode (WE) and metallic lithium foils serving as counter and reference electrodes. The electrodes were immersed in an electrolyte of 1 M LiClO₄ in propylene carbonate and the measurements were taken in an atmosphere containing less than 2 ppm of water. When chronopotentiometry is used to analyze the ion-electron intercalation process, a constant current is applied between the WE and the counter electrode in the direction which drives the ions and electrons into the WE film. The potential, reflecting the energy level at which the ion-electron pairs enter the film, is measured between the WE film and the reference electrode.

Equilibrium chronopotentiometry was performed with an ECO Chemie Autolab/GPES Electrochemical Interface. The current used was only 1 $\mu\text{A}/\text{cm}^2$, which has been shown to be low enough that the measured potential very well represents that of equilibrium [18]. The WE potential was measured in a very wide range of Li/host metal atom ratios, x , in the films. The results are presented by plotting the derivative $-(dx/dU)$, which we denote the “electrochemical density of states,” as a function of the WE film potential.

For amorphous materials, *ab initio* calculations of the electronic structure are limited by the need to take an average over a large number of realizations of the amorphous structure, since the density of states of different realizations of the structure can be substantially different [5]. Computational constraints limit the calculations to relatively small clusters of the material. Therefore we compare our measurements with computations of the electronic structure for crystalline phases of tungsten oxide and titanium oxide. This is not a serious limitation, since the main features in the electronic structure of crystalline and amorphous materials are known to be qualitatively similar [7].

Electronic structure calculations were carried out for the anatase phase of titanium dioxide—the only phase of this material that is able to host a significant number of Li ions—as well as for the monoclinic, tetragonal, and cubic phases of tungsten trioxide by the full-potential linear

muffin-tin-orbital method [19–21]. The calculations were based on the local-density approximation (LDA) and we used the Hedin-Lundqvist [22] parametrization as well as Ceperley-Alder parametrized by Perdew and Zunger [23] for the exchange and correlation potential. Basis functions, electron densities, and potentials were calculated without any geometrical approximation [19–21]. These quantities were expanded in combinations of spherical harmonic functions (with $l_{\max} = 6$) inside nonoverlapping spheres surrounding the atomic sites (muffin-tin spheres) and in a Fourier series in the interstitial region. The muffin-tin sphere occupied approximately 50% of the unit cell. The radial basis functions within the muffin-tin spheres are linear combinations of radial wave functions and their energy derivatives, computed at energies appropriate to their site and principal as well as orbital atomic quantum numbers, whereas outside the muffin-tin spheres the basis functions are combinations of Neuman or Hankel functions [24,25]. In the calculations reported here, we made use of pseudocore $3p$ and valence band $4s$, $4p$, $3d$, and $4f$ basis functions for Ti; pseudocore $5s$, $5p$, and valence band $6s$, $6p$, $5d$, and $5f$ basis functions for W; and valence band $2s$, $2p$, $3d$ basis functions for O with corresponding two sets of energy parameters, one appropriate for the semicore $3p$, $5s$, and $5p$ states, and the other appropriate for the valence states. The resulting basis formed a single, fully hybridizing basis set. This approach has previously proven to give a well-converged basis [19–21]. For sampling the irreducible wedge of the Brillouin zone we used the special k -point method [26,27]. In order to speed up the convergence we have associated each calculated eigenvalue with a Gaussian broadening of width 20 mRy. Because the band gap is usually underestimated by this approximation, we do not expect that the calculations will give accurate values for the absolute energy of, for example, the onset of the conduction band. In the comparison with experiments, we will therefore fit the theoretical and experimental density of states curves to one another, allowing them to be shifted relative to one another on the energy scale.

Figure 1 presents the steady state potential U as a function of Li/W ratio x for crystalline and amorphous WO_3 films. The crystalline film curve exhibits two plateaus at low values of x and one at x values around 1. The two first ones signify transitions from monoclinic to tetragonal and from tetragonal to cubic structure, respectively [18,28]. The curve for the amorphous films starts at a higher potential at $x = 0$ and is very smeared out as a consequence of the disorder. We now study the latter curve in detail. Figure 2 shows the derivative $-dx/dU$ as a function of U for the amorphous WO_3 film. This is a measure of the number of electrons and ions inserted into the material per unit energy. The experimental electrochemical density of states curve has been fitted to the computed density of states of the conduction band of

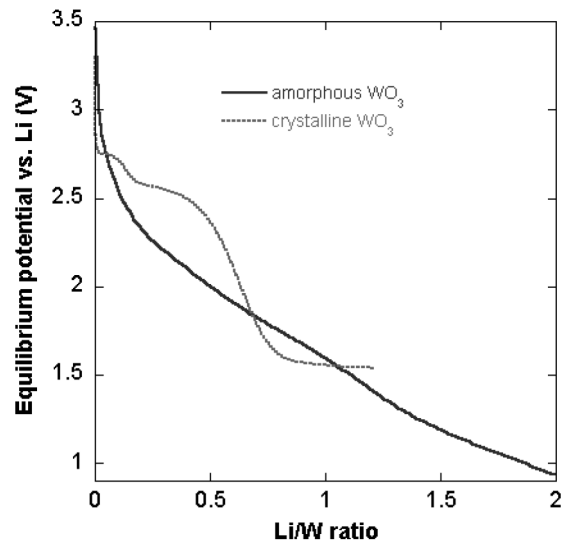


FIG. 1. Equilibrium potential (normalized to the potential of the Li electrode) as a function of the Li/W ratio, x , in polycrystalline (dashed line) and amorphous (solid line) tungsten trioxide films.

monoclinic WO_3 . The shapes of the curves show a remarkable similarity. The relative position of the two pronounced peaks at 1.7 and 2.4 eV is correctly reproduced by the calculations. Differences occur close to the band edge. In the experimental curve there appears to be a band tail extending into the band gap, as expected for a very disordered structure. In addition, band-bending effects, due to the applied bias, might affect the measured density of states in this region. Also the shoulder above

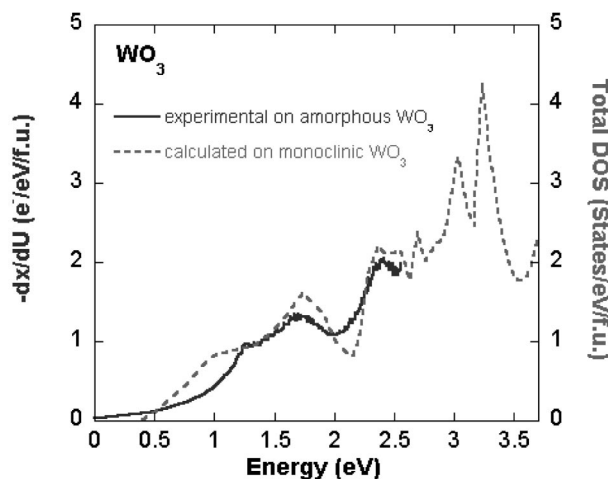


FIG. 2. Electrochemical density of states, $-dx/dU$, for an amorphous WO_3 film (solid line, left scale) and the fitted DOS obtained from band structure calculations for monoclinic WO_3 (dashed line, right scale) are plotted as a function of energy. The zero of energy was taken to be at the experimental band edge, and in the computed total DOS each state can be occupied by two electrons of opposite spin.

the band edge is shifted to higher energies in the experimental curve. The density of states of the tetragonal and cubic phases does not show any similarities with the experimental $-dx/dU$.

Figure 3 shows a comparison between $-dx/dU$ and the computed conduction band density of states of anatase TiO_2 . Again the two major peaks in the experimental curve are in good agreement with the calculations. It is also noted that the experimental curve for the amorphous film exhibits a wide band tail extending into the band gap. As expected, this feature is absent in the computations for the crystalline structure. The range of experiment is set by the achievable level of ion intercalation in the materials; hence the computed high energy features in Figs. 2 and 3 could not be observed.

A formal justification does not exist for interpreting the LDA eigenvalues (for unoccupied states, in particular) as energy eigenvalues of single-electron states. However, this interpretation has been frequently used in the literature [29,30]. By monitoring the sensitivity of the calculated density of states (DOS) to different choices of the exchange and correlation potential, we provide a plausible argument for justifying our use of the LDA eigenvalues. The calculated DOS presented in Figs. 2 and 3 was obtained using the Hedin-Lundqvist exchange and correlation potential [22]. We have also calculated the DOS of TiO_2 using the Ceperley-Alder exchange and correlation potential [23]. The obtained DOS is virtually identical to the one calculated using the Hedin-Lundqvist potential. Thus, our calculated LDA eigenvalues are robust and one can use them in the present situation.

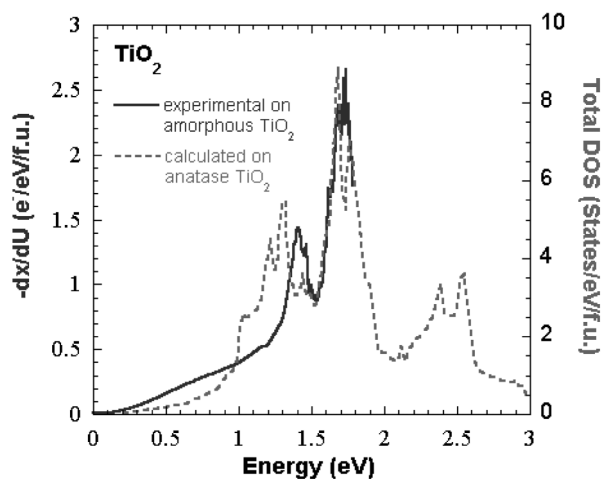


FIG. 3. Electrochemical density of states, $-dx/dU$, for an amorphous TiO_2 film (solid line, left scale) and the fitted DOS obtained from band structure calculations for anatase TiO_2 (dashed line, right scale) are plotted as a function of energy. The zero of energy was taken to be at the experimental band edge, and in the computed total DOS each state can be occupied by two electrons of opposite spin.

The results presented above are completely unexpected. The common understanding of equilibrium potential curves is that their shape is primarily due to a variation in the energies of the sites available for the inserted ions [31]. For example, the curve for amorphous WO_3 in Fig. 1 has earlier been fitted [18] to a model assuming a Gaussian distribution of the energies of the intercalated Li ions [32]. However, such a model cannot reproduce the fine structure seen in the derivative in Fig. 2. The effect of Li intercalation on the electronic band structure has been studied previously from a theoretical point of view. A modification of the rigid-band model to take into account screening of the Li ions by the conduction electrons, originally developed by Friedel [33,34] for alloys, has gained wide acceptance [31]. In this model the Fermi level remains constant as Li is inserted, provided that ion-ion interactions can be neglected, because the whole conduction band is continually translated to lower energies. This means that the equilibrium voltage curves will reflect primarily the energies of the ion sites. Recent *ab initio* calculations of the band structure of MX_2 and LiMX_2 compounds give some support to this picture [35]. In most cases studied, prominent features in the band structure appear at significantly lower energies in the LiMX_2 compounds, although a considerable amount of nonrigid-band behavior was also found together with significant shifts of the Fermi level.

It should be stressed that the theoretical results discussed above were obtained for *crystalline* materials, while the oxide films reported on in Figs. 2 and 3 did not show any sign of crystallinity in x-ray diffraction. For such disordered structures, the lower part of the conduction band should consist of localized states. It is highly probable that the equilibrium voltage curves reflect the shape of the conduction band because of the localized character of the electronic states. In such a situation, it will be energetically favorable for the inserted electron to occupy the localized conduction band state nearest to the Li ion. The interaction energy between the ion and the localized electron will approximately be the same for each newly inserted ion-electron pair; hence the energy distribution of the occupied states should exhibit the shape of the conduction band. In addition, only the portion of electron states in the spatial vicinity of the ion sites will be probed by chronopotentiometry. This may explain a curious feature of the curves in Figs. 2 and 3. Although the shape of the experimental curves corresponds very well with the theoretical density of states, the number of inserted electrons per energy interval is less than the number of states. For WO_3 this difference is a factor of 2, while for TiO_2 it is approximately a factor of 6. These results clearly show that only part of the density of states is probed by our experimental technique. The local coordination in tungsten oxide is based on corner sharing WO_6 octahedra [12], which makes the structure

easily accessible to inserted ions. On the other hand, the anatase local coordination with TiO_6 octahedra sharing two adjacent edges with two other octahedra [12] might make some parts of the structure less accessible to the ions.

In conclusion, we have shown that the fine structure in electrochemical steady state voltage curves displays features in the electronic density of states. The shape of the electrochemical density of states in the conduction band, as observed by chronopotentiometry for amorphous tungsten trioxide and titanium dioxide, was in remarkably good agreement with band structure calculations for the crystalline counterparts. Remaining discrepancies are consistent with expected differences in band structure between amorphous and crystalline structures. The results indicate that the local ordering of the amorphous compounds is monoclinic in the case of WO_3 and anatase in the case of TiO_2 . We propose that localization of the electron states at the Fermi level is a prerequisite for the use of our method. Hence, the method is expected to work for nonmetallic amorphous materials, but not for metals where the electron states have significant itinerant character.

This work was financially supported by a grant from the Swedish Research Council. R. A. also would like to thank the EU network EXC!TING (HPRN-CT-2002-00317) and the Swedish Foundation for Strategic Research (SSF). M. S. would like to thank the Royal Swedish Academy for their support.

*To whom all correspondence should be addressed.

- [1] T. Saito *et al.*, *Science* **300**, 464 (2003).
- [2] H.W. Hugosson *et al.*, *Science* **293**, 2434 (2001).
- [3] L.S. Dubrovinsky *et al.*, *Nature (London)* **410**, 653 (2001).
- [4] P. Sharma *et al.*, *Nat. Mater.* **2**, 673 (2003).
- [5] G. A. de Wijs and R. A. de Groot, *Phys. Rev. B* **60**, 16 463 (1999).
- [6] N. F. Mott and E. A. Davis, *Electronic Processes in Non-Crystalline Materials* (Clarendon, Oxford, 1971).
- [7] S. R. Elliott, *Physics of Amorphous Materials* (Longman, London, 1984).
- [8] I. Pollini, A. Mosser, and J. C. Parlebas, *Phys. Rep.* **355**, 1 (2001).
- [9] C. Main *et al.*, *Solid State Commun.* **83**, 401 (1992).
- [10] J. D. Cohen, D. V. Lang, and J. P. Harbison, *Phys. Rev. Lett.* **45**, 197 (1980).
- [11] G. D. Cody, T. Tiedje, B. Abeles, B. Brooks, and Y. Goldstein, *Phys. Rev. Lett.* **47**, 1480 (1981).
- [12] C. G. Granqvist, *Handbook of Inorganic Electrochromic Materials* (Elsevier, Amsterdam, 2002), 2nd ed.
- [13] C. Bechinger *et al.*, *Nature (London)* **383**, 608 (1996).
- [14] M. Grätzel, *Nature (London)* **409**, 575 (2001).
- [15] M. Wagemaker, A. P. M. Kentgens, and F. M. Mulder, *Nature (London)* **418**, 397 (2002).
- [16] About 300 nm thick films of tungsten trioxide and titanium dioxide were deposited by dc magnetron sputtering from metallic W (99.95%) and Ti (99.9%) targets, respectively, onto unheated electrically conducting In_2O_3 :Sn substrates in an atmosphere of argon and oxygen. The total pressure during sputtering was 30 mTorr for the case of tungsten and 60 mTorr for the case of titanium. The oxygen/argon ratios in the gas were 1.25 and 0.086, respectively. Other details about the sputtering conditions are given in A. Azens *et al.*, *Appl. Phys. Lett.* **68**, 3701 (1996); *J. Appl. Phys.* **78**, 1968 (1995). For comparison purposes, films of crystalline tungsten trioxide were deposited by heating the substrates to 350 °C during the deposition.
- [17] X-ray diffraction, using a Siemens D 5000 diffractometer with a CuK_α cathode, showed that the films deposited onto unheated substrates were x-ray amorphous, while the crystalline tungsten trioxide films were found to be monoclinic with a grain size of ~ 50 nm, as obtained from peak profile fittings using Scherrer's equation [18].
- [18] M. Strømme Mattsson, *Phys. Rev. B* **58**, 11015 (1998).
- [19] L. S. Dubrovinsky *et al.*, *Nature (London)* **388**, 362 (1997).
- [20] J. M. Wills and B. R. Cooper, *Phys. Rev. B* **36**, 3809 (1987).
- [21] D. L. Price and B. R. Cooper, *Phys. Rev. B* **39**, 4945 (1989).
- [22] L. Hedin and B. I. Lundqvist, *J. Phys. C* **4**, 2064 (1971).
- [23] D. M. Ceperley and B. J. Alder, *Phys. Rev. Lett.* **45**, 566 (1980); J. P. Perdew and A. Zunger, *Phys. Rev. B* **23**, 5048 (1981).
- [24] O. K. Andersen, *Phys. Rev. B* **12**, 3060 (1975).
- [25] H. L. Skriver, *The LMTO Method* (Springer, Berlin, 1984).
- [26] D. J. Chadi and M. L. Cohen, *Phys. Rev. B* **8**, 5747 (1973).
- [27] S. Froyen, *Phys. Rev. B* **39**, 3168 (1989).
- [28] Q. Zhong, J. R. Dahn, and K. Colbow, *Phys. Rev. B* **46**, 2554 (1992).
- [29] W. Kohn, *Rev. Mod. Phys.* **71**, 1253 (1999).
- [30] U. von Barth, *Phys. Scr.* **T109**, 9 (2004).
- [31] W. R. McKinnon, in *Solid State Electrochemistry*, edited by P. G. Bruce (Cambridge University Press, Cambridge, 1995), pp. 163–198.
- [32] T. Kudo and M. Hibino, *Solid State Ionics* **84**, 65 (1996).
- [33] J. Friedel, *Adv. Phys.* **3**, 446 (1954).
- [34] D. J. Sellmyer, *Solid State Phys.* **33**, 83 (1978).
- [35] M. K. Aydinol *et al.*, *Phys. Rev. B* **56**, 1354 (1997).